

# Optimisation of variables for studying Higgs boson transverse momentum distributions in the $H \rightarrow b\bar{b}$ decay mode

Summer student : Yuekai Hu

Supervisor: Xingguo Li

September 4th, 2019

## Abstract

The large Higgs transverse momentum greater than 175 GeV is sensitive to loop effects from presence of Beyond Standard Model heavy new particles<sup>[1]</sup>. This report focuses on optimization of observables to probe the Higgs transverse momentum in the  $H \rightarrow b\bar{b}$  production in association with a Z boson. The measurement of these optimized observables at hadron colliders can significantly increase sensitivities to new physics.

## 1 Introduction

The  $Z/\gamma^*$  transverse momentum in the Drell-Yan process, in which a quark and an anti-quark annihilates to form  $Z/\gamma^*$  and then decay to an lepton/anti-lepton pair, is limited by the experimental resolution of the lepton transverse momenta. The transverse momentum arises due to radiations of gluons and quarks from incoming partons. Optimisation of variables to probe the  $Z/\gamma^*$  transverse momentum has been performed in this context<sup>[2]</sup>.

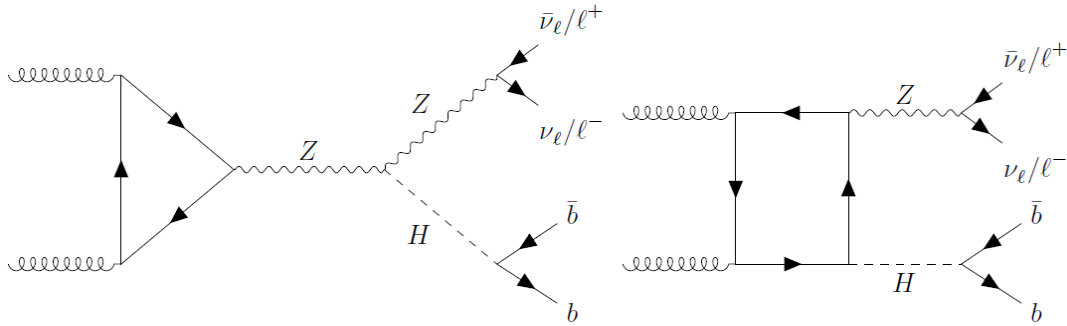


Figure 1 The Feynman diagrams of  $H \rightarrow b\bar{b}$  decay mode in ZH production. The analysis considers only the Z decaying into di-leptons case.

The  $H \rightarrow b\bar{b}$  production in association with a  $W/Z$  boson has been observed with the ATLAS detector<sup>[3]</sup>. For Higgs transverse momentum greater than 175 GeV (top mass), presence of Beyond Standard Model (BSM) heavy particles can distort Higgs transverse momentum, thus finding suitable variables with better resolution for studying Higgs transverse momentum is of great importance to increase sensitivities to new physics.

This project applies the state-of-the-art technique proposed in the Drell-Yan process to  $pp \rightarrow ZH \rightarrow l^+l^-b\bar{b}$  ( $l$  can be  $e$  or  $\mu$ ) channel to find the best variable that probe the large Higgs transverse momentum.

## 2 Event selection

In this analysis, we use a  $ZH$  sample at truth level and apply appropriate smearing to the truth lepton/jets full vector to mimic the detector effects. In order to mimic the selection of  $H \rightarrow b\bar{b}$  produced along with a  $Z$  boson at the detector level, events are required to satisfy the following selection criteria. The decay products must contain at least two  $b$  jets. Also, for the selected  $b$  jet, events were excluded if either of the transverse momentum of the  $b$  jet is smaller than 25 GeV. Simultaneously, the modulus pseudo-rapidity of both jets should be smaller than 2.5. The study only considers jets which are well separated.

For leptons, both the transverse momentum of di-leptons should be larger than 25 GeV, and the modulus pseudo-rapidity of di-leptons should be smaller than 2.5.

## 3 Candidate observables to probe Higgs transverse momentum

We introduce five new variables apart from the total transverse momentum of two objects,  $Q_t$  or  $p_t$ .

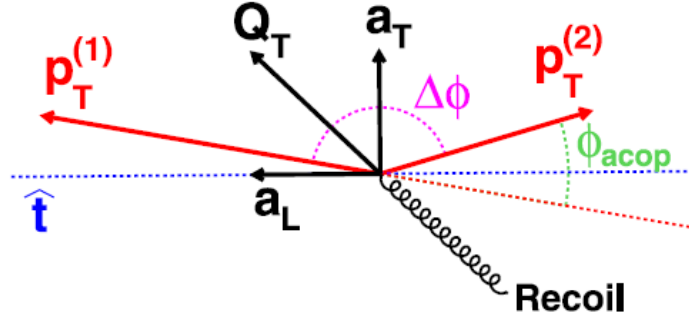


Figure 2 A schematic demonstration of observables in the plane that is transverse to the beam direction<sup>[3]</sup>

Figure 2 is the plane transverse to the beam direction and shows the definition of the new variables.  $Q_t$  is the transverse momentum of the di-b-jets / di-leptons.  $\Delta\phi$  is the angle between the two transverse momentum of di-b-jets/di-leptons, and its acoplanarity angle is  $\phi_{acop}$ . The thrust axis is defined as  $\hat{t} = (p_t^{(1)} - p_t^{(2)})/|p_t^{(1)} - p_t^{(2)}|$ , and  $Q_t$  is split into two components with regard to the thrust axis, the parallel component, denoted by  $a_L$ , and the orthogonal component,  $a_t$ .

In order to cancel the effect of lepton/jets transverse momentum resolution,  $a_t$  and  $Q_t$  can be divided by the invariant mass of di-b-jets,  $Q$ , thus forming two variables  $a_t/Q$  and  $Q_t/Q$ .

Since the lepton/jet angular resolution is much better than that of the transverse momentum, two angular variables,  $\phi_\eta^*$  and  $\tan(\phi_{acop}/2)$  are introduced to mitigate the effect of transverse momentum resolution.  $\phi_\eta^*$  is defined as  $\phi_\eta^* \equiv \tan(\phi_{acop}/2) \sin(\theta_\eta^*)$ , where  $\cos(\theta_\eta^*) = \tanh(\frac{\eta^- - \eta^+}{2})$  is the cosine value of the scattering angle and  $\eta$  is the pseudorapidity of a jet or lepton.

In order to compare the variable resolution, scaling of the new variables is applied such that it has a unit of GeV. Since  $a_t$  is one of the two components of the transverse momentum, all variables concerning  $a_t$  is scaled by  $\sqrt{2}$ . And  $a_t/Q$ ,  $Q_t/Q$ ,  $\phi_\eta^*$ ,  $\tan(\phi_{acop}/2)$  should all be scaled by the mass to get the same unit as the transverse momentum. For  $\tan(\phi_{acop}/2)$ , since the mean value of  $\sin(\theta^*)$  is  $\sim 0.85$ , so it has an additional scaling factor of 0.85.

#### 4 Mythology

In order to mimic the detector effects, Gaussian Smearing is applied to the lepton and jet truth transverse momentum,  $\eta$ ,  $\phi$ .

The resolution of the jet transverse momentum is calorimeter-like and takes the following form ,

$\sigma_{Pt}/Pt = \sqrt{(\frac{A}{Pt})^2 + (\frac{B}{\sqrt{Pt}})^2 + C^2}$ , where A is the noise term, B is the stochastic part and C is a constant. The specific value of the factors A, B, C in each event is dependent on  $\eta$ . For electrons , the resolution of the transverse momentum takes the for  $\sigma_{Pt} = \sqrt{(0.01 \times Pt)^2 + (0.99)^2}$ , and for muons,  $\sigma_{Pt} = 1\% \times Pt + 0.00014\% \times (Pt)^3$ .

The resolutions of  $\eta$  and  $\phi$  for leptons are better than jets. For jets, it takes the form  $\sigma =$

$$\sqrt{(0.37\%)^2 + (\frac{0.544}{Pt})^2}. \text{ And for leptons, } \sigma = \sqrt{(0.036\%)^2 + (\frac{0.013}{Pt})^2}.$$

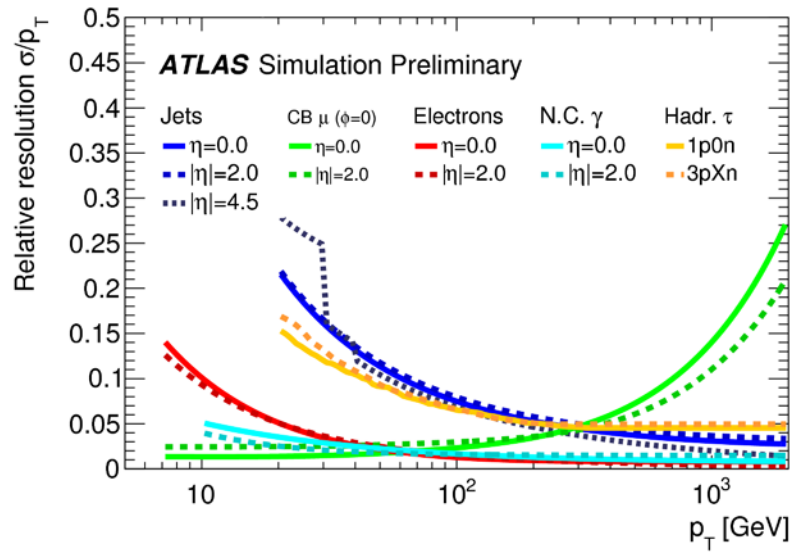


Figure 3 Relative transverse momentum resolution of stable particles at the ATLAS experiment<sup>[4]</sup>

As is shown in Figure 3, for transverse momentum less than 100 GeV, the relative resolution of muon is the best, around 1—3%. For the jet resolution, which is at least 10%, is much worse than that of di-leptons. However, as the transverse momentum increases, the muon resolution rises sharply, whereas the electron and jet resolution declines. For transverse momentum at approximately 1000 GeV, the resolution of jet, dominated by the constant term, is much better than muon but worse than electron.

The distribution of the transverse momentum,  $\eta$  and  $\phi$  of di-b-jets (Figure 4), di-electrons (Figure 6), di-muons (Figure 8) before and after smearing is shown below. Also, the distribution of newly introduced variables  $a_t$ ,  $a_t/Q$ ,  $Q_t/Q$ ,  $\phi_\eta^*$ ,  $\tan(\phi_{acop}/2)$  that respectively using the smeared and unsmeared transverse momentum,  $\eta$  and  $\phi$  of di-b-jets (Figure 5), di-electrons (Figure 6), di-muons

(Figure 8) are also shown below. It can be observed from the graphs that the peak of mass after smearing is about the half of that before smearing and the difference of transverse momentum before and after smearing is around 5% , which is as expected and self-assuring.

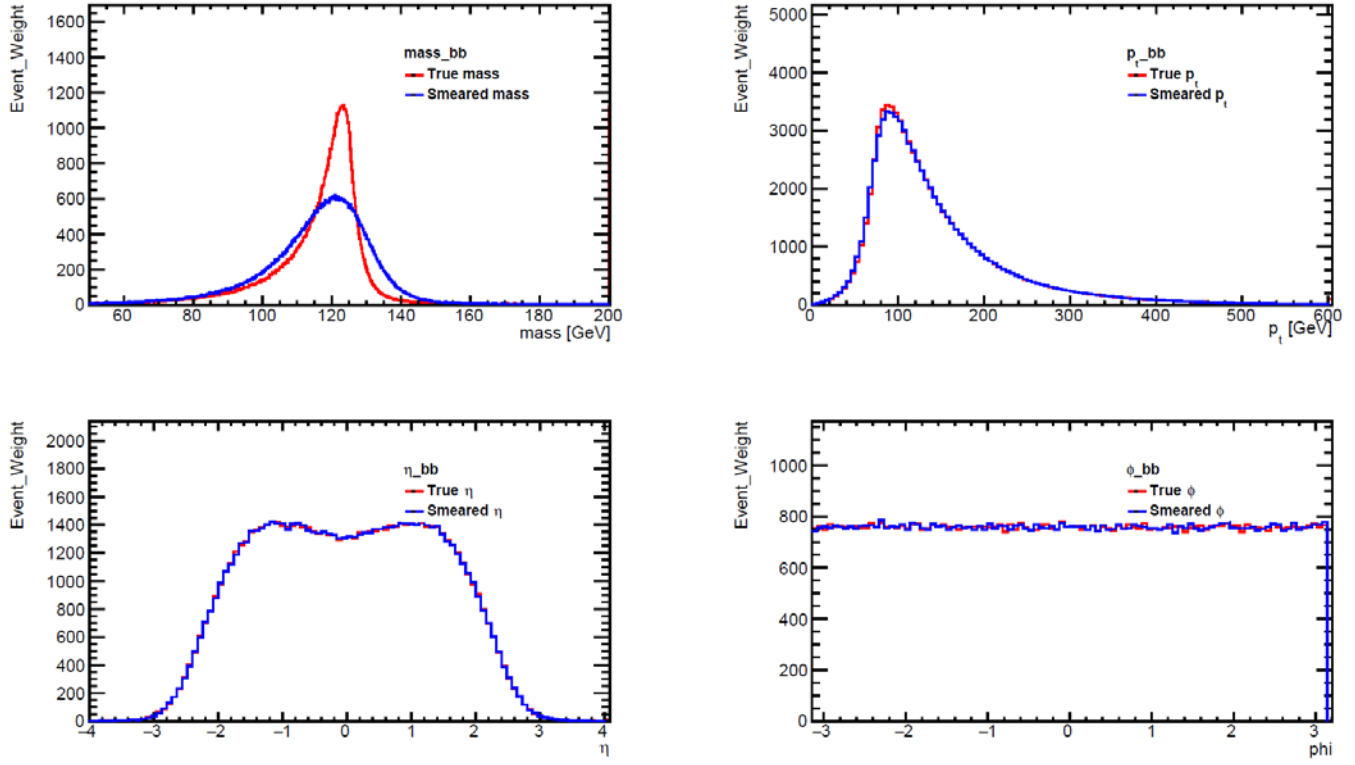


Figure 4 The truth and smeared observable distributions for di-b-jets

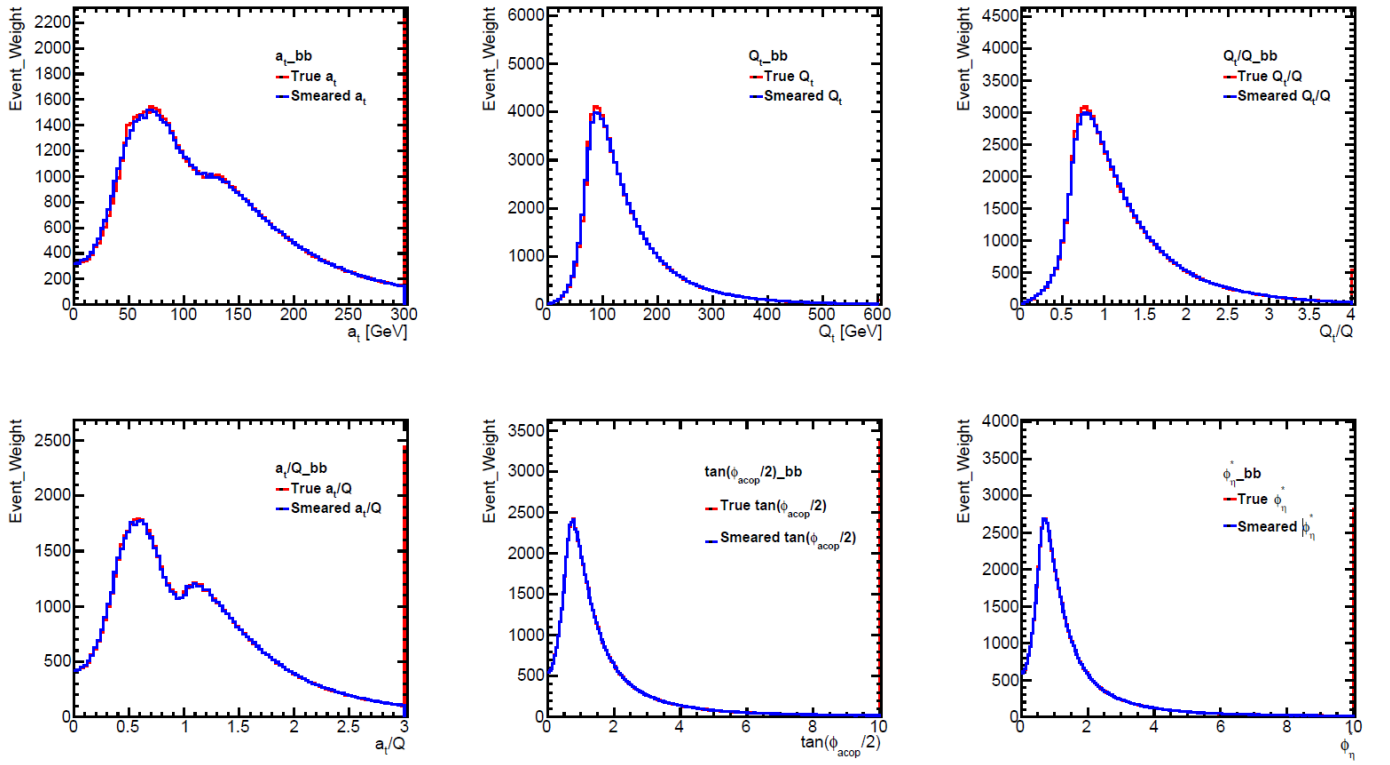


Figure 5 The truth and smeared new variables of di-b-jets

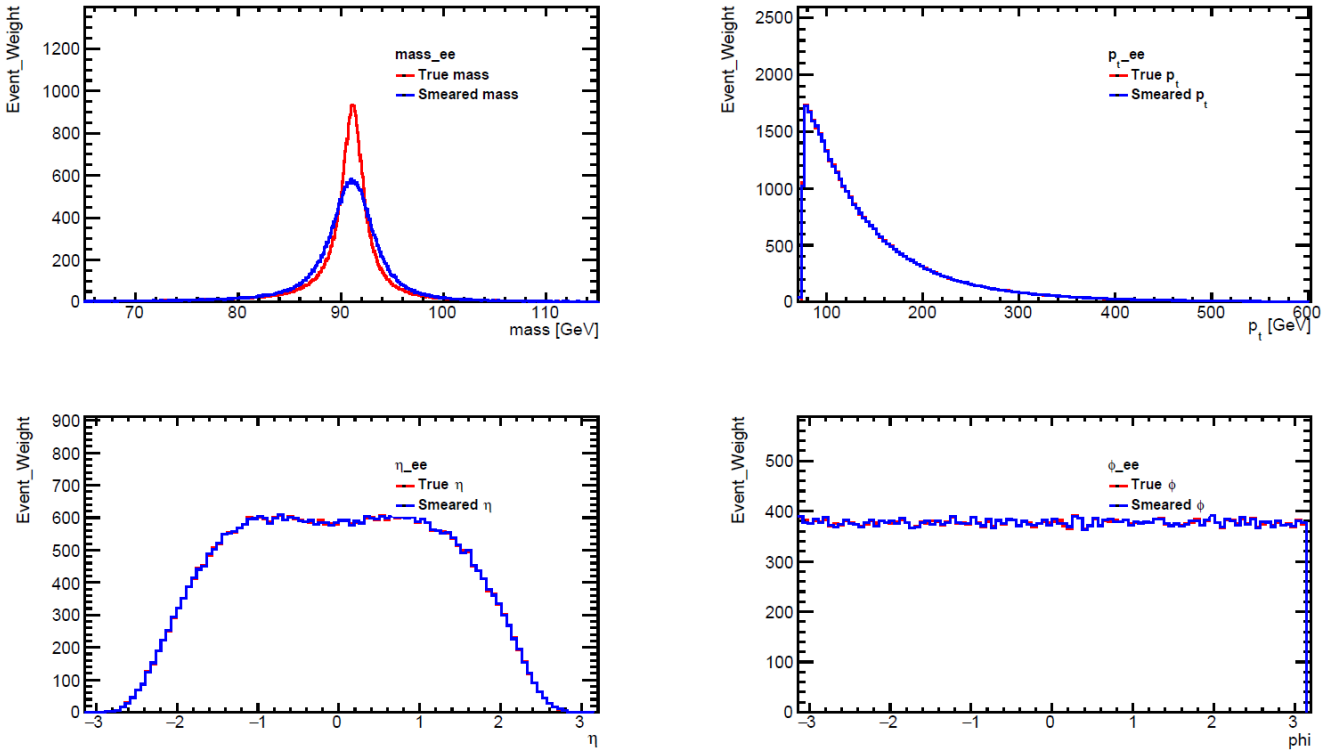


Figure 6 The truth and smeared observable distributions for di-electrons

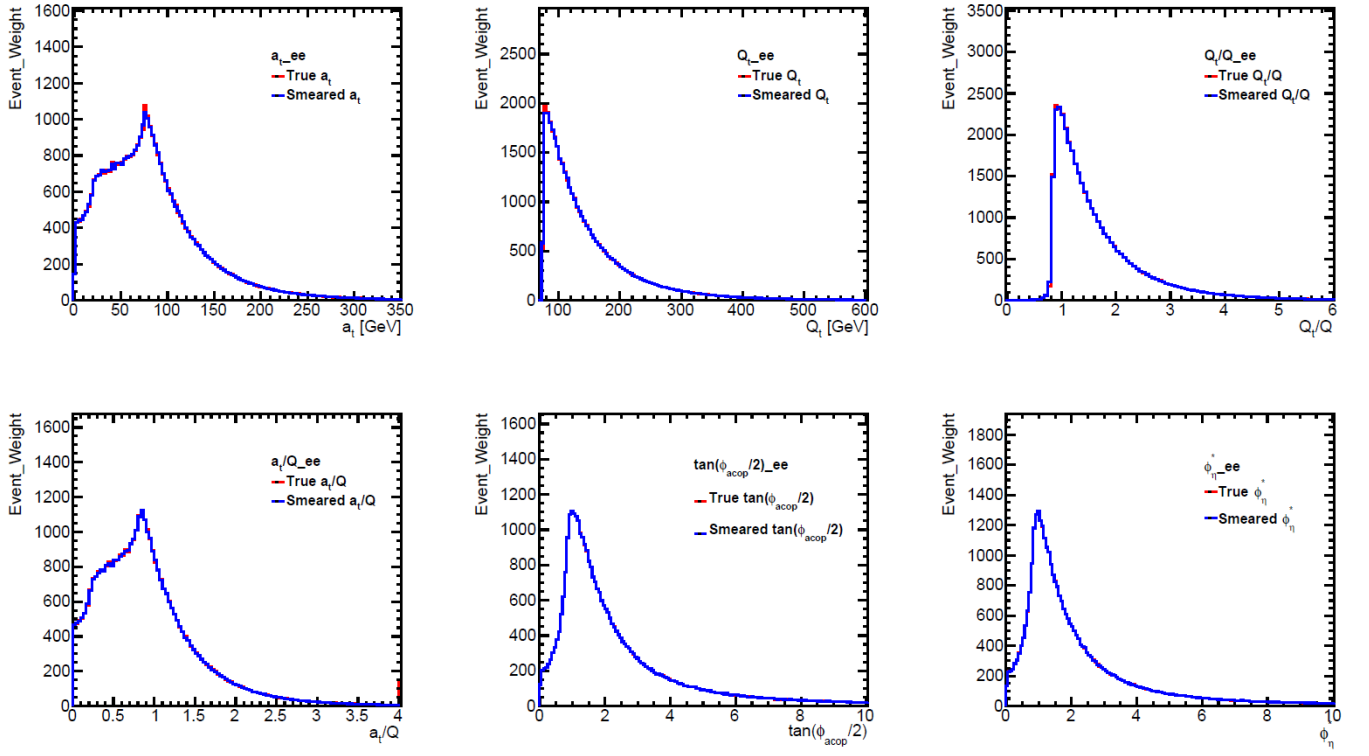


Figure 7 The truth and smeared new variables of di-electrons

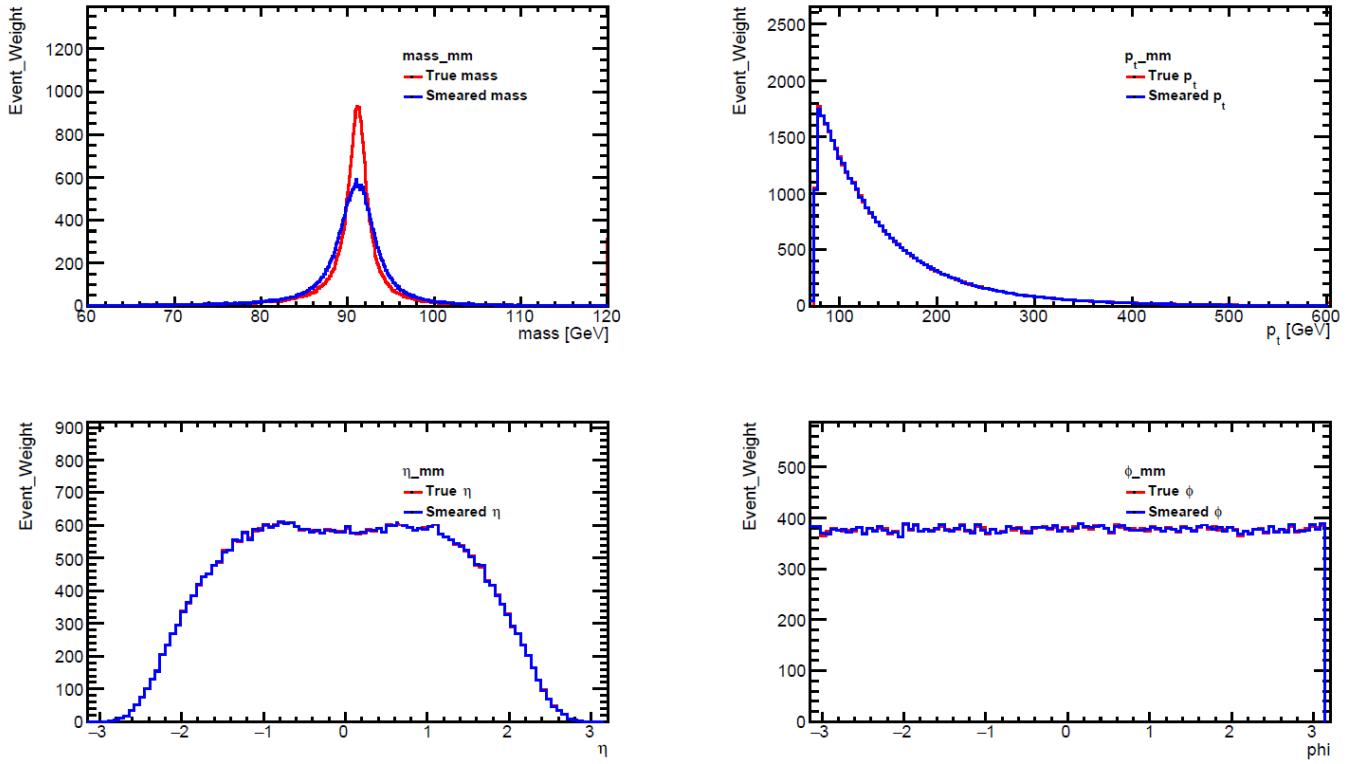


Figure 8 The truth and smeared observable distributions for di-muons

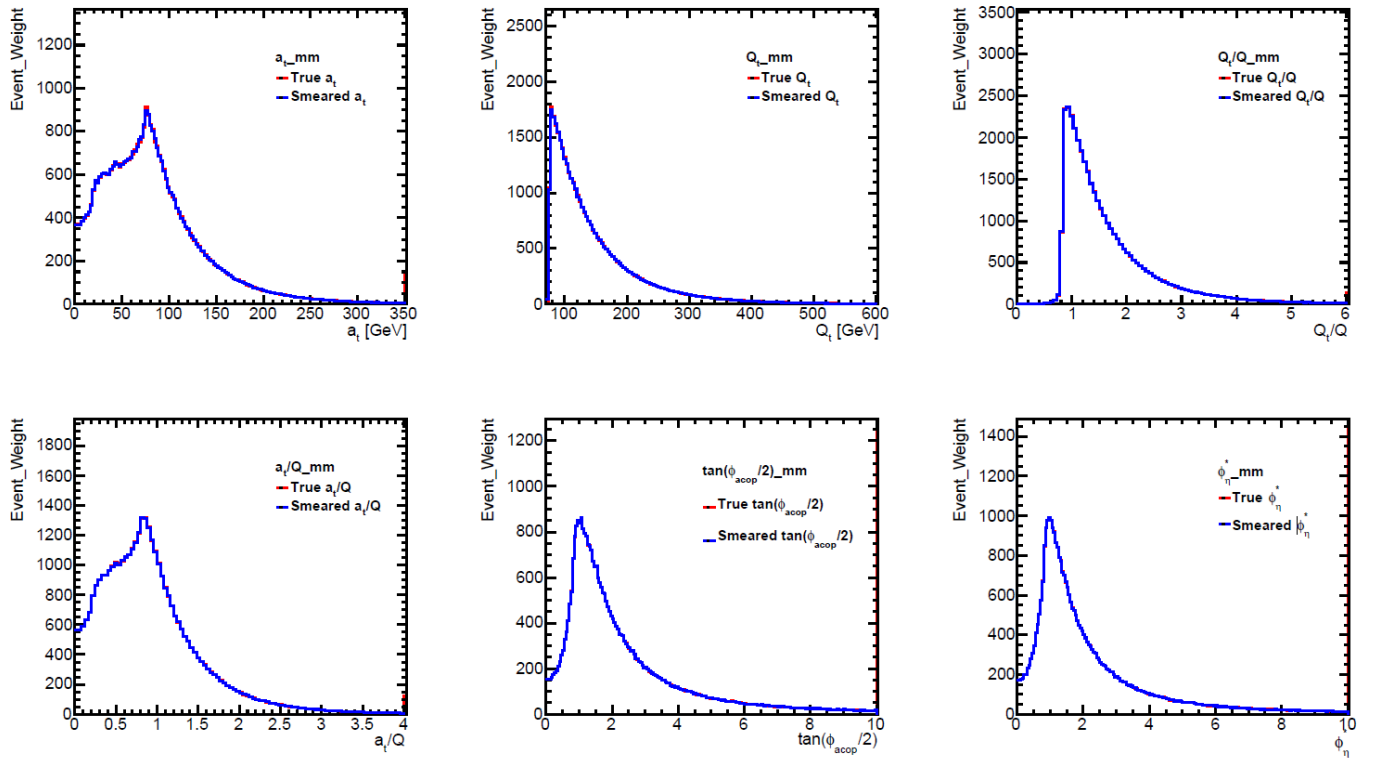


Figure 9 The truth and smeared new variables of di-muons



## 5 Results

The distribution of the resolution between smeared and truth variables  $a_t$ ,  $a_t/Q$ ,  $Q_t/Q$ ,  $\phi_{\eta}^*$ ,  $\tan(\phi_{acop}/2)$  of di-b-jets, di-electrons and di-muons are shown in Figure 10, 11, 12, respectively.

Figure 10 shows the comparison of the resolution of the variables before and after smearing of b jets. As is shown in Figure 10 the resolution of  $a_t/Q$  and  $Q_t/Q$  are the best and the angular variable resolution is comparable.

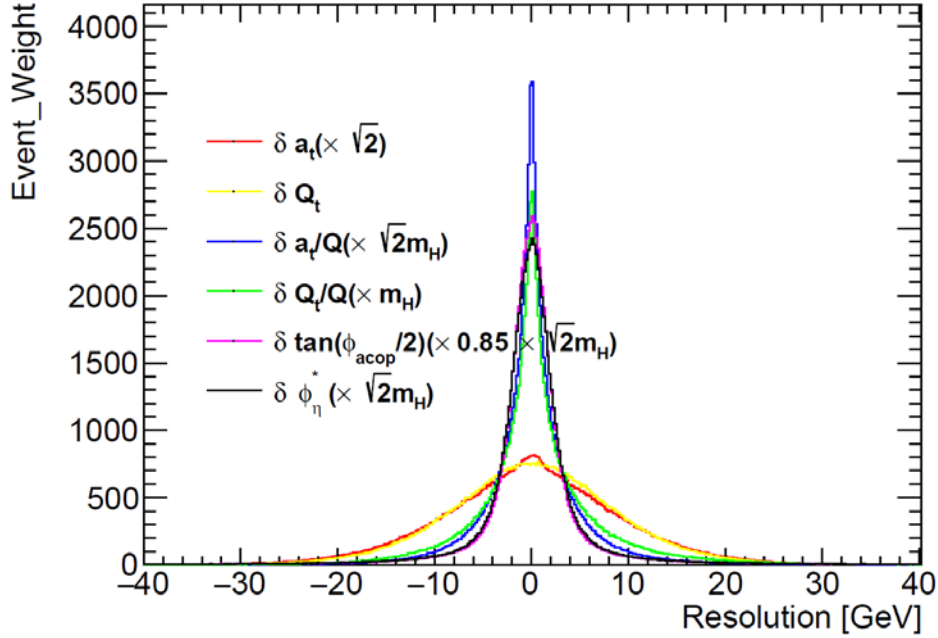


Figure 10 The distribution of the resolutions of variables before and after smearing of di-b-jets

Figure 11 shows the distribution of the variables before and after smearing of electron full vector. The resolutions of all variables  $a_t$ ,  $a_t/Q$ ,  $Q_t/Q$ ,  $\phi_{\eta}^*$ ,  $\tan(\phi_{acop}/2)$  are all better than those of di-b-jets, because the resolutions of the transverse momentum,  $\eta$  and  $\phi$  of electrons used in Gaussian smearing is much better than that of jets. The resolutions of angular variable here are the best, the resolution of  $a_t/Q$  and  $Q_t/Q$  is in between, and the  $a_t$  resolution is the worst.

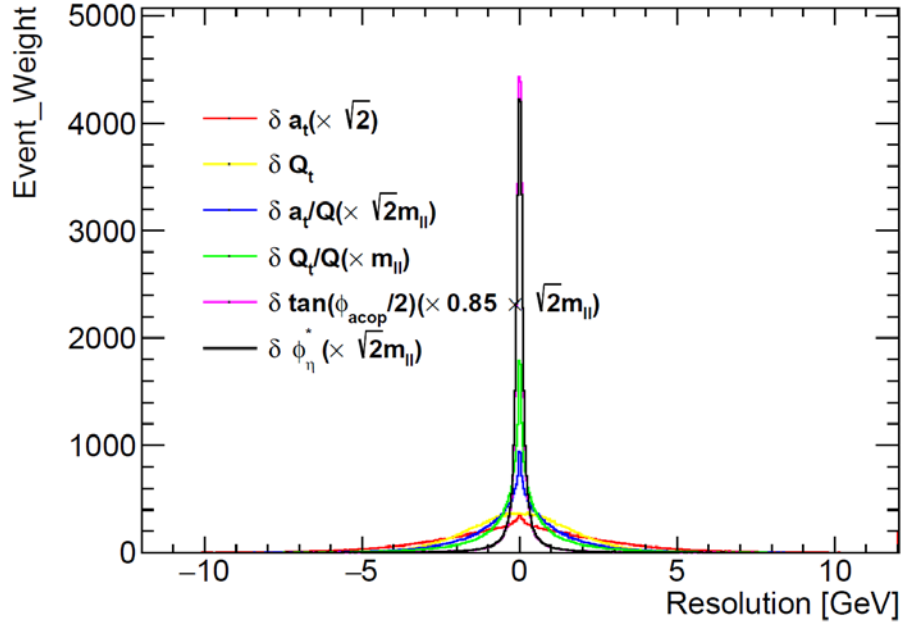


Figure 11 The distribution of the resolutions of variables before and after smearing for di-electrons

Figure 12 shows the distribution of the variables before and after smearing of di-muons. The resolutions of all variables  $a_t$ ,  $a_t/Q$ ,  $Q_t/Q$ ,  $\phi_\eta^*$ ,  $\tan(\phi_{acop}/2)$  are all better than those of di-b-jets, but worse than those of dielectron, because the resolutions of the transverse momentum,  $\eta$  and  $\phi$  of muons used in Gaussian smearing is much better than those of bjets, but not as good as those of electrons. The resolutions of angular variables here are the best, the resolution of  $a_t/Q$  and  $Q_t/Q$  is in between, and the  $a_t$  resolution is the worst.

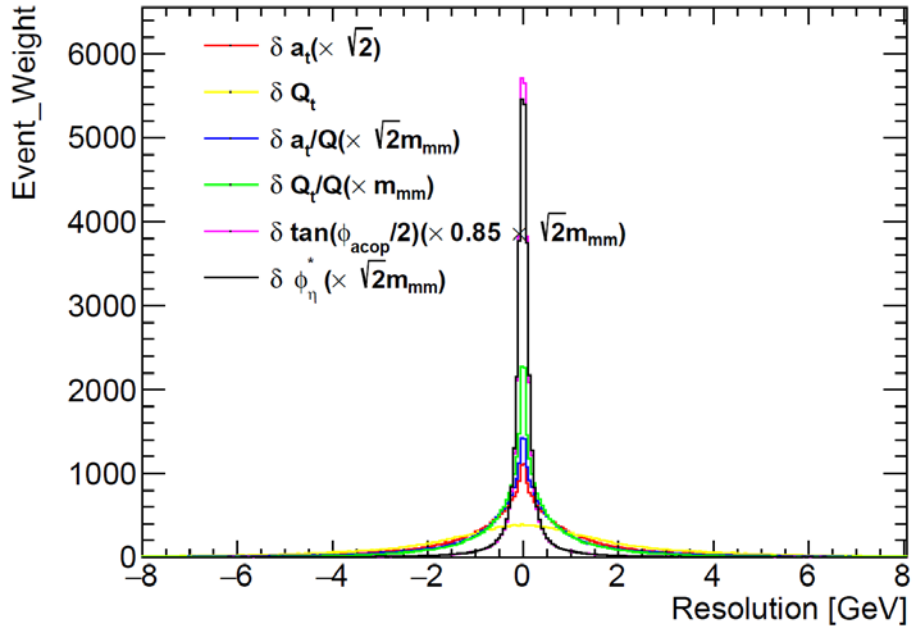


Figure 12 The distribution of the resolutions of variables before and after smearing of di-muons

The resolution is determined in terms of the scaled variables. As plotted in Figure 13,14,15 ,the resolutions increase with the scaled variables i.e. the Higgs transverse momentum.

Figure 13 shows the resolution of different variables of di-b-jets. For the Higgs transverse momentum lower than 500 GeV, the angular variables have the best resolutions.  $a_t$  and  $Q_t$  are the worst and  $a_t/Q$  and  $Q_t/Q$  are in between. For Higgs transverse momentum between 500 GeV and 700 GeV, the resolution of angular variables,  $a_t/Q$  and  $Q_t/Q$  are almost the same. For Higgs transverse momentum higher than 700 GeV, the resolutions of all variables are very close to each other, where the constant terms in jet resolution becomes dominant.

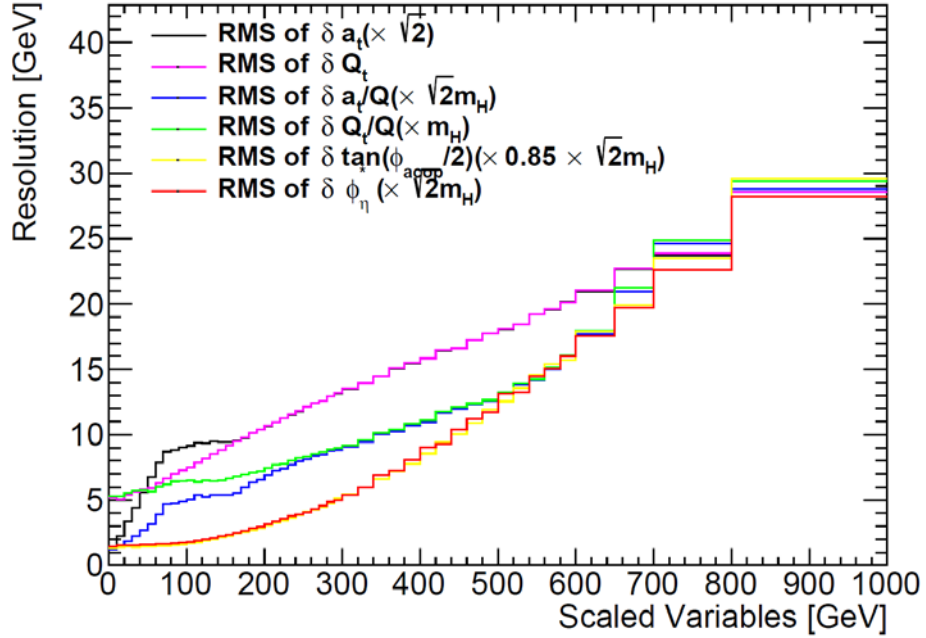


Figure 13 Resolution of the scaled variable as a function of itself for di-b-jets

Figure 14 shows the resolution of different variables of di-electrons. For the Z boson transverse momentum from 0 to 1000 GeV, the resolutions of angular variables are always the best, followed by the resolution of  $Q_t/Q$ ,  $Q_t$ ,  $a_t/Q$ , and the resolution of  $a_t$  is the worst. Compared with the resolution of all variables of di-b-jets, those of di-electrons are much better.

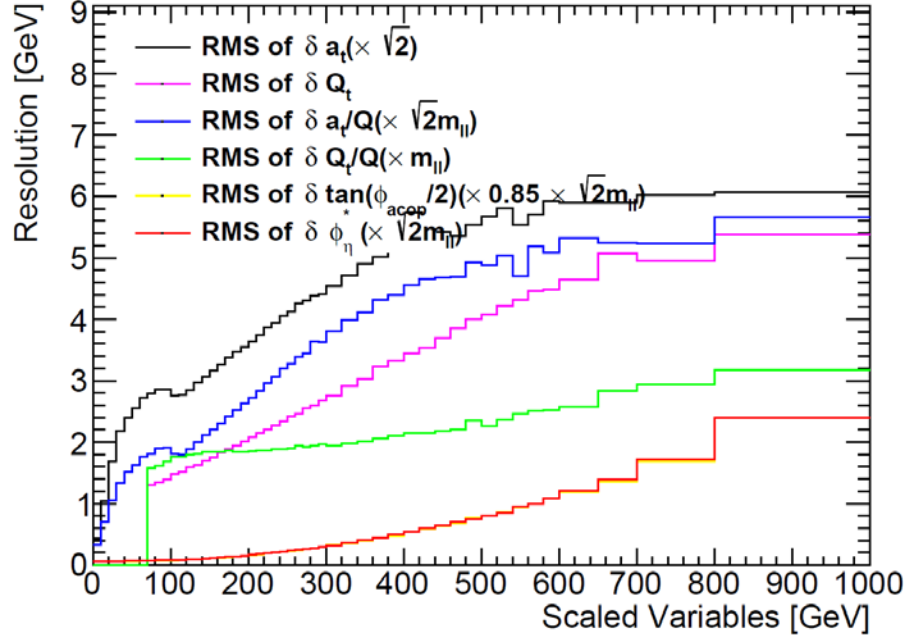


Figure 14 Resolution of the scaled variable as a function of itself for di-electrons

Figure 15 shows the resolution of different variables of di-muons. For the Z boson transverse momentum from 0 to 800 GeV, the resolutions of angular variables are always the best, followed by the resolution of  $Q_t/Q$ ,  $a_t/Q$ ,  $a_t$ , and the resolution of  $Q_t$  is the worst. Compared with the resolutions of all variables of di-b-jets, those of di-muons are better, but are not as good as those of di-electrons.

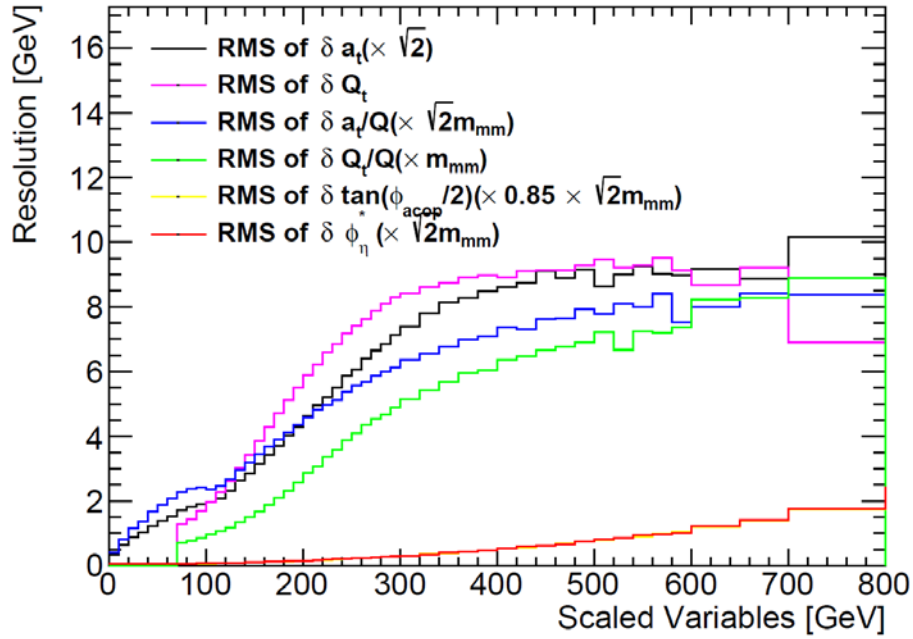


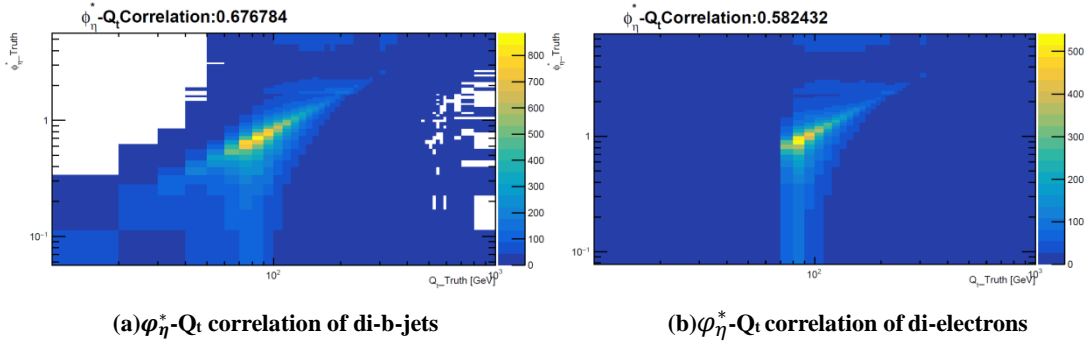
Figure 15 Resolution of the scaled variable as a function of itself for di-muons

To decide which variable of  $a_t$ ,  $a_t/Q$ ,  $Q_t/Q$ ,  $\phi_\eta^*$ ,  $\tan(\phi_{acop}/2)$  is the optimized variable to probe Higgs transverse momentum, the correlation between these variables and the Higgs transverse momentum need to be determined to ensure the variables can be used to probe the large Higgs transverse momentum.

Figure 16 shows the correlation between  $\phi_\eta^*$  and the transverse momentum,  $Q_t$  for di-b-jets(a), di-electrons(b), di-muons(c), and the  $\phi_\eta^*-\phi_\eta^*$  correlation of di-leptons and di-b-jets(d). And shown in the figure, since  $\phi_\eta^*$  are sensitive to the low Higgs transverse momentum below 125 GeV with four times better resolution than using b jet transverse momentum. It is much less susceptible to Higgs transverse momentum larger than 200 GeV. Therefore,  $\phi_\eta^*$  is not a suitable variable to probe Higgs transverse momentum greater than 175 GeV.

The scaled variables  $a_t/Q$  and  $Q_t/Q$  in the dilepton system in the  $ZH \rightarrow l^+l^-b\bar{b}$  channel are the best variables to study Higgs transverse momentum larger than 125 GeV based on the observable resolution as well as the correlation with the Higgs transverse momentum.

The correlations of  $\tan(\phi_{acop}/2)$ , behaves similarly as  $\phi_\eta^*$ , is insufficient to probe Higgs transverse momentum greater than 125 GeV, and additional correlation plots between different variables can be found in the Appendix.



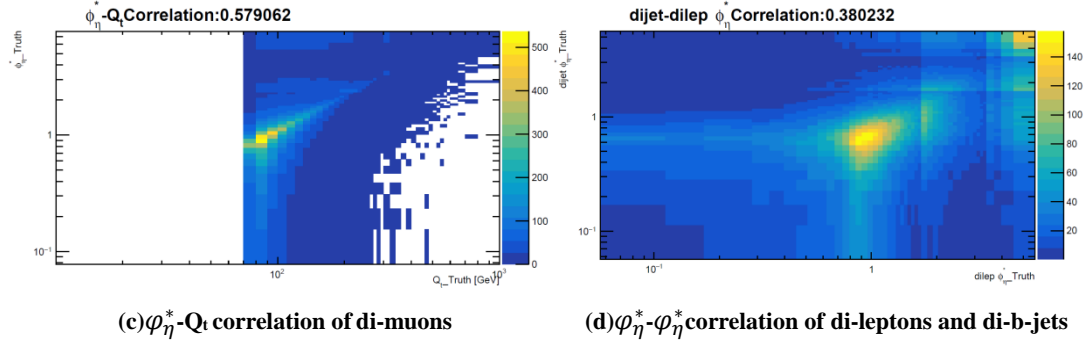


Figure16 The correlation concerning  $\phi_{\eta^*}$

Figure17 shows the correlations between  $Q_t/Q$  and the transverse momentum of di-b-jets(a), di-electrons(b), di-muons(c), and the  $Q_t/Q$  - $Q_t/Q$  correlation between di-leptons and di-b-jets(d).

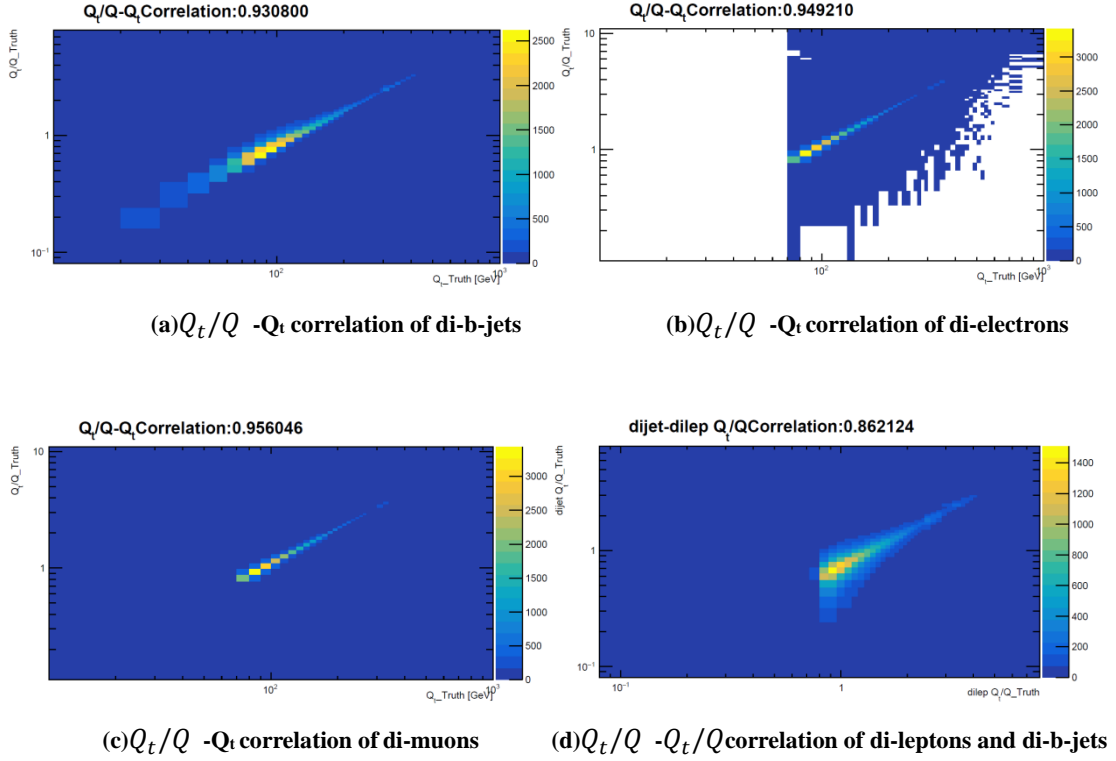


Figure17 The correlation concerning  $Q_t/Q$

## 6 Conclusion

The project investigates the best observable to study the large Higgs transverse momentum sensitive to the presence of BSM heavy particles. The angular variables  $\phi_{\eta^*}$  and  $\tan(\phi_{acop}/2)$  are sensitive to Higgs transverse momentum below Higgs mass ( $\sim 125$  GeV). For Higgs transverse momentum

above the Higgs mass,  $a_t/Q$  and  $Q_t/Q$  are the optimised variables. In particular, for  $ZH$  channel, the  $Z$  boson can be used to probe the Higgs transverse momentum. Therefore, measurement of  $a_t/Q$  and  $Q_t/Q$  for both Higgs and  $Z$  bosons are important in improving sensitivities to new physics. For the other  $VH$  channels with 1 or 0 lepton in the final state,  $a_t/Q$  and  $Q_t/Q$  in the di-b-jets system are the best variables to study the Higgs transverse momentum.

## Acknowledgements

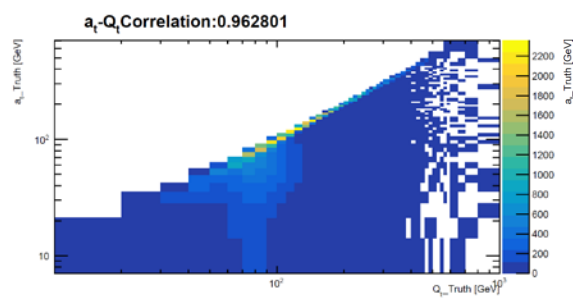
The author and her supervisor want to express their gratitude to Stephen Jiggins from Friedberg University for providing the truth Ntuples for this analysis.

## Reference

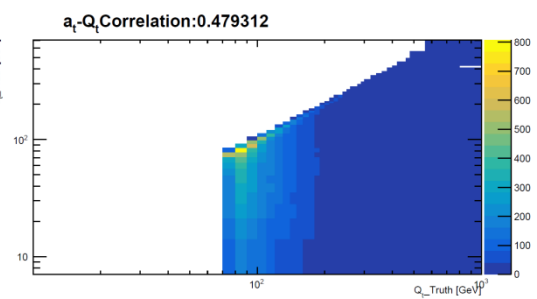
- [1] Massimiliano Grazzini, Agnieszka Ilnicka, Michael Spira, Marius Wiesemann PoS(EPS-HEP2015) 144
- [2] A. Banfi, S. Redford, M. Vesterinen, P. Waller, T.R. Wyatt, Eur. Phys. J. C 71:1600(2011)
- [3] ATLAS Collaboration, Physics Letters B 786(2018)59–86
- [4] ATLAS Collaboration, ATLAS-CONF-2018-038

## Appendix

correlation plots between different variables

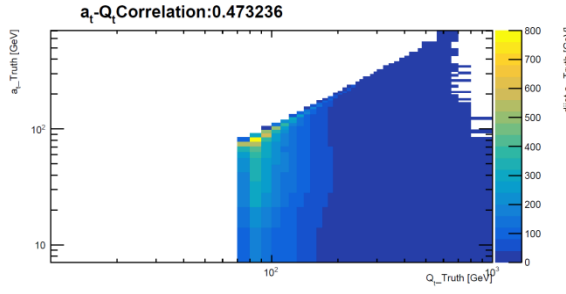


$a_t$ - $Q_t$  correlation of di-b-jets

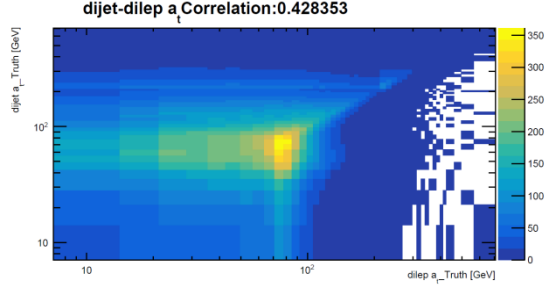


$a_t$ - $Q_t$  correlation of di-electrons

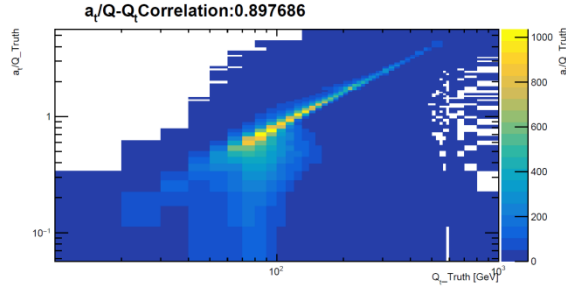




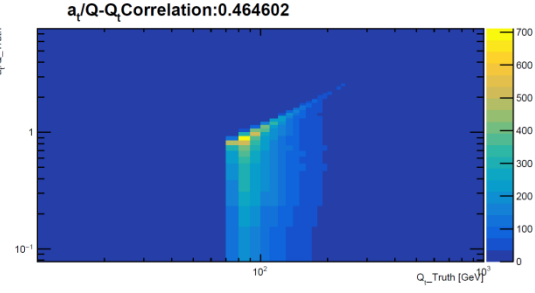
**$a_t$ - $Q_t$  correlation of di-muons**



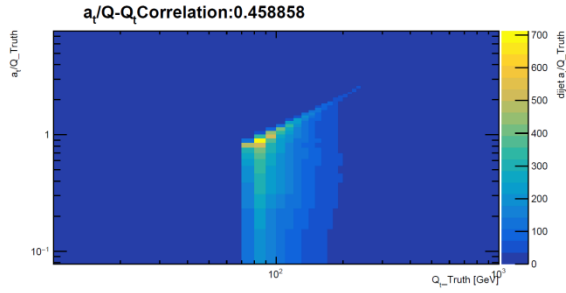
**$a_t$ - $a_t$  correlation of di-leptons and di-b-jets**



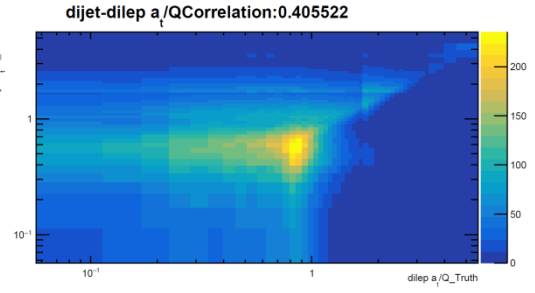
**$a_t/Q$  - $Q_t$  correlation of di-b-jets**



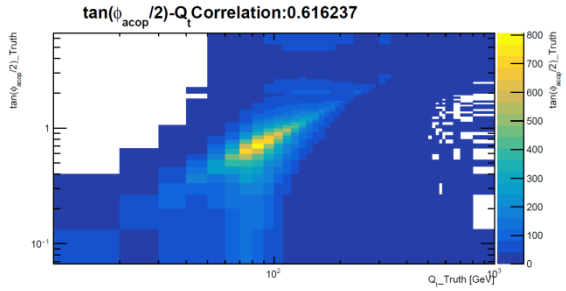
**$a_t/Q$  - $Q_t$  correlation of di-electrons**



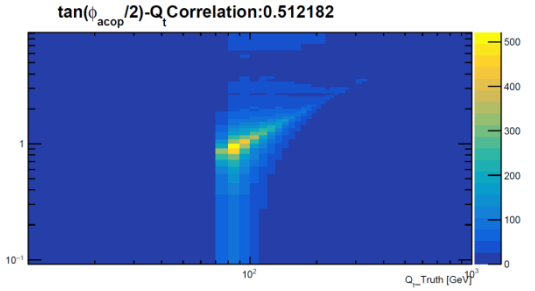
**$a_t/Q$  - $Q_t$  correlation of di-muons**



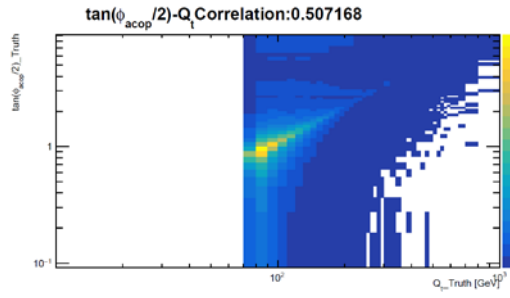
**$a_t/Q$  - $a_t/Q$  correlation of di-leptons and di-b-jets**



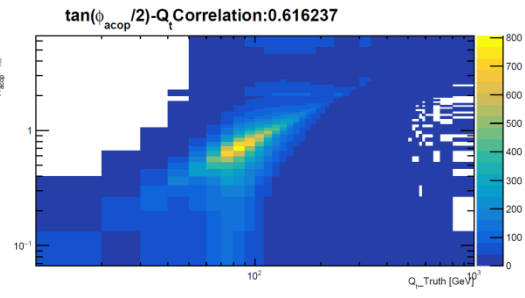
**$\tan(\phi_{acop}/2)$  - $Q_t$  correlation of di-b-jets**



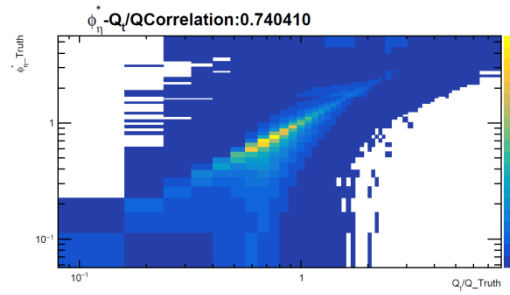
**$\tan(\phi_{acop}/2)$  - $Q_t$  correlation of di-electrons**



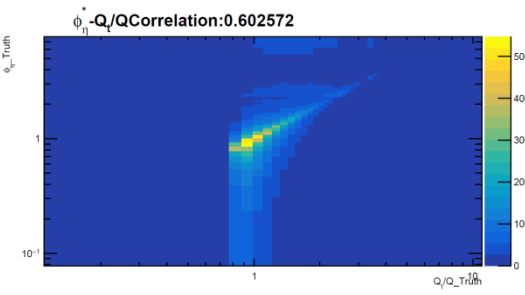
$\tan(\phi_{acop}/2)$  - $Q_t$  correlation of di-muons  
jets



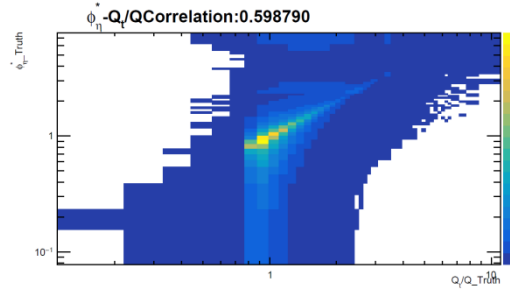
$\tan(\phi_{acop}/2)$  correlation of di-leptons and di-b-



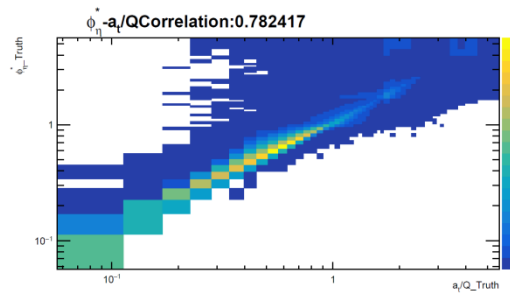
$\phi_{\eta}^*$ - $Q_t/Q$  correlation of di-b-jets



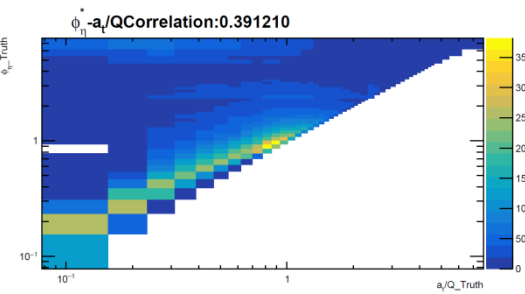
$\phi_{\eta}^*$ - $Q_t/Q$  correlation of di-electrons



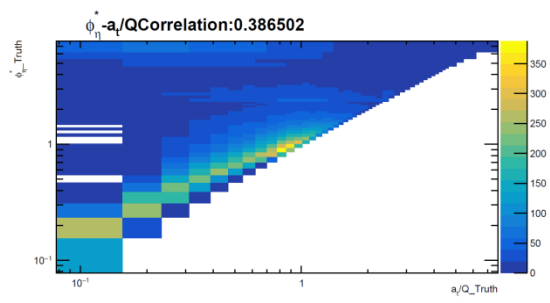
$\phi_{\eta}^*$ - $Q_t/Q$  correlation of di-muons



$\phi_{\eta}^*$ - $a_t/Q$  correlation of di-b-jets



$\phi_{\eta}^*$ - $a_t/Q$  correlation of di-electrons



$\phi_\eta^* - a_t/Q$  correlation of di-muons